

# Biodistribution and pharmacokinetics of $^{188}\text{Re}$ -liposomes and their comparative therapeutic efficacy with 5-fluorouracil in C26 colonic peritoneal carcinomatosis mice

Chia-Che Tsai<sup>1</sup>  
 Chih-Hsien Chang<sup>1</sup>  
 Liang-Cheng Chen<sup>1</sup>  
 Ya-Jen Chang<sup>1</sup>  
 Keng-Li Lan<sup>2</sup>  
 Yu-Hsien Wu<sup>1</sup>  
 Chin-Wei Hsu<sup>1</sup>  
 I-Hsiang Liu<sup>1</sup>  
 Chung-Li Ho<sup>1</sup>  
 Wan-Chi Lee<sup>1</sup>  
 Hsiao-Chiang Ni<sup>1</sup>  
 Tsui-Jung Chang<sup>1</sup>  
 Gann Ting<sup>3</sup>  
 Te-Wei Lee<sup>1</sup>

<sup>1</sup>Institute of Nuclear Energy Research, Taoyuan, <sup>2</sup>Cancer Center, Taipei Veterans General Hospital, Taipei, <sup>3</sup>National Health Research Institutes, Taipei, Taiwan, ROC

Correspondence: Te-Wei Lee  
 Institute of Nuclear Energy Research,  
 1000 Wenhua Road, Chian Village,  
 Lungtan, Taoyuan, Taiwan, ROC  
 Tel +886 3 4711400  
 Fax +886-3-4711416  
 Email twlee@iner.gov.tw

**Background:** Nanoliposomes are designed as carriers capable of packaging drugs through passive targeting tumor sites by enhanced permeability and retention (EPR) effects. In the present study the biodistribution, pharmacokinetics, micro single-photon emission computed tomography (micro-SPECT/CT) image, dosimetry, and therapeutic efficacy of  $^{188}\text{Re}$ -labeled nanoliposomes ( $^{188}\text{Re}$ -liposomes) in a C26 colonic peritoneal carcinomatosis mouse model were evaluated.

**Methods:** Colon carcinoma peritoneal metastatic BALB/c mice were intravenously administered  $^{188}\text{Re}$ -liposomes. Biodistribution and micro-SPECT/CT imaging were performed to determine the drug profile and targeting efficiency of  $^{188}\text{Re}$ -liposomes. Pharmacokinetics study was described by a noncompartmental model. The OLINDA|EXM<sup>®</sup> computer program was used for the dosimetry evaluation. For therapeutic efficacy, the survival, tumor, and ascites inhibition of mice after treatment with  $^{188}\text{Re}$ -liposomes and 5-fluorouracil (5-FU), respectively, were evaluated and compared.

**Results:** In biodistribution, the highest uptake of  $^{188}\text{Re}$ -liposomes in tumor tissues ( $7.91\% \pm 2.02\%$  of the injected dose per gram of tissue [ $\%ID/g$ ]) and a high tumor to muscle ratio ( $25.8 \pm 6.1$ ) were observed at 24 hours after intravenous administration. The pharmacokinetics of  $^{188}\text{Re}$ -liposomes showed high circulation time and high bioavailability (mean residence time [MRT] = 19.2 hours, area under the curve [AUC] =  $820.4\%ID/g \cdot h$ ). Micro-SPECT/CT imaging of  $^{188}\text{Re}$ -liposomes showed a high uptake and targeting in ascites, liver, spleen, and tumor. The results were correlated with images from autoradiography and biodistribution data. Dosimetry study revealed that the  $^{188}\text{Re}$ -liposomes did not cause high absorbed doses in normal tissue but did in small tumors. Radiotherapeutics with  $^{188}\text{Re}$ -liposomes provided better survival time (increased by 34.6% of life span;  $P < 0.05$ ), tumor and ascites inhibition (decreased by 63.4% and 83.3% at 7 days after treatment;  $P < 0.05$ ) in mice compared with chemotherapeutics of 5-fluorouracil (5-FU).

**Conclusion:** The use of  $^{188}\text{Re}$ -liposomes for passively targeted tumor therapy had greater therapeutic effect than the currently clinically applied chemotherapeutics drug 5-FU in a colonic peritoneal carcinomatosis mouse model. This result suggests that  $^{188}\text{Re}$ -liposomes have potential benefit and are safe in treating peritoneal carcinomatosis of colon cancer.

**Keywords:** biodistribution, dosimetry, 5-fluorouracil, micro-SPECT/CT,  $^{188}\text{Re}$ -liposomes

## Introduction

Colorectal cancer is one of the most common types of cancer in men and women. Its prognosis depends on the extent of the disease and only about 40% of patients

with colorectal cancers are diagnosed at the early stage.<sup>1</sup> At this stage, surgical tumor resection is the main method of treatment and the 5-year survival rate of patients can reach 90%. If the cancer has progressed, there is lymph node involvement and development of hematogenous metastases, so that prognosis becomes poor.<sup>2</sup> Peritoneal dissemination is considered the terminal stage in colorectal cancer. “Peritoneal carcinomatosis” means extensive or widespread dissemination of tumor nodules inside the abdomen. Certain sites in the abdomen are more prone to implantation of tumor cells, including the greater omentum, the hepatic hilum, the mesentery, the pelvis, and the peritoneum covering the diaphragm.<sup>3,4</sup> Peritoneal carcinomatosis is also the most common cause of malignant ascites; the production and leakage of fluid from the malignant cells causes exudation of extracellular fluid into the peritoneal cavity, in turn causing discomfort, pain, and symptoms that diminish the quality of life for cancer patients.<sup>5</sup>

The treatment of peritoneal or distant metastasis from colorectal cancer remains a challenging problem.<sup>2</sup> For several decades, regimens based on 5-fluorouracil (5-FU) have been the first choice for primary or adjuvant chemotherapy for colorectal cancer.<sup>6,7</sup> 5-FU belongs to the family of drugs called “antimetabolites” and works through noncompetitive inhibition of thymidylate synthase. In clinical standard care for first-line therapy, patients with metastatic colorectal cancer receiving systemic chemotherapy of 5-FU and leucovorin have a median survival that is increased from approximately 6 months to about 12 months.<sup>7</sup> In recent years, a number of new treatments have become available for patients with advanced colorectal cancer. The effectiveness of these drugs has been compared with that of 5-FU in clinical studies.<sup>2,8</sup> However, no effective therapy for peritoneal metastasis is yet available, though novel agents remain under investigation. In preclinical drug development, 5-FU also serves as the comparative object to evaluate the anticancer efficacy for colon cancer.<sup>9,10</sup>

Several therapeutics based on nanoparticles have been successfully introduced for cancer treatment. The first generation of nanoparticles is primarily based on liposomes and polymer-drug conjugates.<sup>11</sup> Nanoliposomes are double-membrane lipid vesicles capable of packaging drugs for various delivery applications. Nanopegylated liposomes can evade the reticuloendothelial system and remain in the circulation for prolonged periods, improving tumor targeting and efficacy in animal models. Nanopegylated liposomes provide passive targeting because of nanoliposome accumulation in tumors by means of the enhanced permeability and retention (EPR)

effect through leaky tumor vasculature.<sup>12,13</sup> Preclinical studies have shown that cytotoxic agents entrapped in pegylated liposomes tend to accumulate in tumors.<sup>14,15</sup> A prominent example is pegylated liposomal doxorubicin, which has been applied in patients with acquired immune deficiency syndrome-related Kaposi's sarcoma (ARKS), as well as ovarian, breast, and prostate carcinomas.<sup>16–18</sup>

Preclinical studies of tumor therapy with radionuclide-liposome conjugates or liposome-mediated radiotherapeutics have been reported.<sup>19</sup> Rhenium-188 (<sup>188</sup>Re) is a radionuclide used for imaging and therapeutic dual applications due to its short physical half-life of 16.9 hours with 155 keV gamma emissions for imaging, and its 2.12 MeV  $\beta$  emission with a maximum tissue penetration range of 11 mm for tumor therapeutics. In addition, <sup>188</sup>Re can be obtained from commercial nuclear generators, which makes it convenient for routine research and clinical use.<sup>20</sup>

In this study, the biodistribution, pharmacokinetics, and micro single-photon emission computed tomography (micro-SPECT/CT) imaging of intravenous injection of <sup>188</sup>Re-liposomes were investigated in a C26 colonic peritoneal carcinomatosis mouse model. The therapeutic efficacy of <sup>188</sup>Re-liposomes was compared with that of 5-FU. The experimental goals were to demonstrate the potential applications of nanotargeted <sup>188</sup>Re-liposomes via an intravenous route for internal radiotherapy of peritoneal carcinomatosis and ascites.

## Materials and methods

### Materials

Pegylated liposomes (Nano-X) were provided by Taiwan Liposome Company (Taipei, Taiwan). The tungsten-188 (<sup>188</sup>W)/<sup>188</sup>Re generator was purchased from Oak Ridge National Laboratory (Oak Ridge, TN). Elution of the <sup>188</sup>W/<sup>188</sup>Re generator with normal saline provided solutions of carrier-free <sup>188</sup>Re as sodium perrhenate (NaReO<sub>4</sub>). N,N-bis(2-mercaptoethyl)-N',N'-diethylethylenediamine (BMEDA) were purchased from ABX (Radeberg, Germany). The C26 murine colon carcinoma cell line was obtained from the American Type Culture Collection (Manassas, VA). Stannous chloride (SnCl<sub>2</sub>) was purchased from MERCK (Darmstadt, Germany). The PD-10 column was purchased from GE Healthcare (Uppsala, Sweden). All other chemicals were purchased from MERCK.

### Cell culture and animal tumor ascites model

C26 murine colon carcinoma cell line was obtained from the American Type Culture Collection (Manassas).

It was grown in Roswell Park Memorial Institute medium-1640 supplemented with 10% (v/v) fetal bovine serum, 2 mM L-glutamine at 37°C in 5% CO<sub>2</sub>. Male BALB/c mice were obtained from the National Laboratory Animal Center, Taipei, Taiwan. Mice were housed in a controlled environment, with food and water provided ad libitum. One hundred and seventy-one mice (6–8 weeks old) were inoculated intraperitoneally with  $2 \times 10^5$  C26 cells in 500  $\mu$ L phosphate-buffered saline. Mice were sacrificed by CO<sub>2</sub> asphyxiation at the desired time points after tumor inoculation. The abdominal cavity was carefully inspected and all ascites and tumor nodules were meticulously collected and weighed. Animal protocols were approved by the Institutional Animal Care and Use Committee at the Institute of Nuclear Energy Research, Taiwan.

### Preparation of <sup>188</sup>Re-BMEDA-labeled pegylated liposomes (<sup>188</sup>Re-liposomes)

The pegylated liposomes (Nano-X) were prepared according to the method described by Tseng et al.<sup>21</sup> The lipid compositions of liposome contain hydrogen soybean phosphatidylcholine (HSPC), cholesterol, polyethylene glycol-(1,2-distearoyl-sn-glycero-3-phosphatidylethanolamine) (PEG-DSPE; molar ratio 3:2:0.3) and ammonium sulfate solution with [250 mM (NH<sub>4</sub>)<sub>2</sub>SO<sub>4</sub>, pH 5.0] in the inner water phase. Pegylated nanoliposomes have an average particle size of about 82.59 nm and contain 13.16  $\mu$ mol/mL phospholipids.

The method for radiolabeling BMEDA with <sup>188</sup>Re was as has been previously described.<sup>22</sup> Briefly, BMEDA (ABX), stannous chloride was used as the reductant and glucoheptonate (Sigma-Aldrich, St Louis, MO) was used as an intermediate ligand to make <sup>188</sup>Re-SNS/S complexes. Five milligrams of BMEDA were pipetted into a fresh vial. A volume of 0.5 mL of 0.17 mol/L glucoheptonate dissolved in a 10% acetate solution was added, followed by the addition of 120  $\mu$ L (10  $\mu$ g/ $\mu$ L) of stannous chloride. After flushing the solution with N<sub>2</sub> gas, highly specific activity of <sup>188</sup>Re-sodium perrhenate was added. The vial was sealed and heated in an 80°C water bath for 1 hour. The labeling efficiency of <sup>188</sup>Re-BMEDA complexes was analyzed by silica gel-impregnated glass fiber sheets using normal saline as the developer.

The Nano-X pegylated liposomes (1 mL) were added to the <sup>188</sup>Re-BMEDA (50–250 MBq) solution and incubated at 60°C for 30 minutes. The <sup>188</sup>Re-liposomes were separated from free <sup>188</sup>Re-BMEDA using a PD-10 column eluted with normal saline. Each 0.5 mL fraction was collected into a tube. The opacity of pegylated liposomes was used to visually

monitor the collection of the <sup>188</sup>Re-liposomes. The labeling efficiency was determined using the activity in pegylated liposomes after separation, divided by the total activity before separation.

### Biodistribution and pharmacokinetic studies

Thirty-five C26 colon peritoneal metastatic carcinoma-bearing mice (22–26 g, average weight 24.6 g) received an intravenous injection of 3.7 MBq/200  $\mu$ L of <sup>188</sup>Re-liposomes with 0.88  $\mu$ mol phospholipid for biodistribution and pharmacokinetic studies. Mice were kept on a 12-hour day/night cycle and had free access to food and water. For biodistribution study, 30 mice were sacrificed by CO<sub>2</sub> asphyxiation, five mice each at 1, 4, 16, 24, 48, and 72 hours after administration. At each time point, the organs of interest were sampled and whole organs collected where possible. The samples were rinsed in saline, blotted dry, weighed, and then counted using a Packard Cobra II Auto-Gamma (PerkinElmer, Inc, Waltham, MA) counter. Samples of the injection of <sup>188</sup>Re-liposomes were used as decay correction standards. Data were expressed as percent of the injected dose (ID) per gram of tissue (%ID/g).

For pharmacokinetics, blood samples of 20 to 100  $\mu$ L were collected at 0.083 (5 minutes), 0.5, 1, 4, 16, 24, 48, 72, 120, and 168 hours from five mice via heart puncture after intravenous injection of <sup>188</sup>Re-liposomes (20  $\mu$ L at 0.083, 0.5, 1, 4, 16, 24 hours; 50  $\mu$ L at 48, 72, 120 hours; 100  $\mu$ L at 168 hours). Concentrations of radioactivity in the blood were expressed as %ID/mL. Pharmacokinetic parameters were determined using WinNonlin (v 5.0.1; Pharsight Corp, Mountain View, CA) software. Noncompartmental analysis model 200 (extravascular input) was used with the Log/linear trapezoidal rule. Parameters, including terminal half-life ( $T_{1/2\lambda_z}$ ),  $T_{max}$ ,  $C_{max}$ , total body clearance (Cl) and area under the curve (AUC) were determined. Pharmacokinetic parameters associated with the terminal phase were calculated using the best-fit method to estimate the terminal half-life.

### Micro-SPECT/CT imaging and whole-body autoradiography (WBAR)

For micro-SPECT/CT imaging, three mice received an intravenous injection of 12.95 MBq/200  $\mu$ L of <sup>188</sup>Re-liposomes and 0.88  $\mu$ mol phospholipid. The mice were anesthetized with 1.5% isoflurine (positioned prone in the scanner) and received micro-SPECT/CT imaging at 72 hours after intravenous injection. SPECT and CT images were acquired

using a micro-SPECT/CT scanner (X-SPECT/CT, Gamma Medica, Northridge, CA). The SPECT images were acquired using a parallel hole collimator, with the center of the field of view (FOV) focused on the abdomen of each mouse. The radius of rotation was 1 cm with an FOV of 1.37 cm. The imaging was accomplished using 64 projections at 60 seconds per projection. SPECT imaging was followed by CT image acquisition (X-ray source: 50 kVp, 0.4 mA; 256 projections). The software provided with the X-SPECT/CT scanner was used for the SPECT and CT image reconstruction including the SPECT/CT image fusion. SPECT images were reconstructed to produce image sizes of  $56 \times 56 \times 56$  pixels with an image resolution of 1.2 mm. CT images were also reconstructed in image sizes of  $512 \times 512 \times 512$  pixels with 0.15 mm image resolution.

The procedure for WBAR has been previously described. Mice were sacrificed by CO<sub>2</sub> euthanasia at 72 hours after micro-SPECT/CT imaging and were immediately dipped into liquid nitrogen. The frozen carcasses were then embedded with 2.5% carboxymethyl cellulose and the frozen carboxymethyl cellulose block was attached to the sample stage in the cryochamber (−20°C). After resting for 2 hours, the frozen sample was then sectioned (into slices 40 μm thick) using a cryomicrotome (CM 3600; Leica Microsystems GmbH, Wetzlar, Germany) at −20°C. These samples were placed in contact with an imaging plate (BAS-MS 2040; Fuji Photo Film Co) for 5 days. After completing the exposure, the imaging plate was analyzed with a FLA-5100 (Fuji Photo Film Co) reader and the Multi Gauge v 3.0 (Fuji Photo Film Co) software.

## Absorbed radiation dose calculations

To estimate mean absorbed doses in humans, the relative organ mass scaling method was used. The mean absorbed dose in various tissues is derived from the radionuclide concentration in tissues/organs of interest, assuming a homogeneous distribution of the radionuclide within any source region. The calculated mean value of %IA/g for the organs in mice was extrapolated to uptake in organs of a 70 kg adult using the formula:

$$\left[ \left( \frac{\%IA}{g} \right)_{\text{organ}}^{\text{animal}} \times (kg_{\text{TBweight}})^{\text{animal}} \right] \times \left( \frac{g_{\text{organ}}}{kg_{\text{TBweight}}} \right)_{\text{human}} = (\%IA/\text{organ})_{\text{human}}$$

The extrapolated values (%IA) in human organs at 1, 4, 16, 24, 48, and 72 hours were fitted with exponential biokinetic models and integrated to obtain the number of disintegrations in the source organs; this information was entered into the OLINDA|EXM® (v 1.0; Vanderbilt University, Nashville, TN) program. The integrals (MBq-s) for 14 organs, including

heart contents (blood), brain, muscle, bone, heart, lung, testes, spleen, pancreas, kidneys, liver, stomach, small intestine, lower intestine, and remainder of the body, were evaluated and used for the dosimetry evaluation.

For excretion study, mice were kept in metabolic cages and urine and feces were collected at various time intervals. Cumulative excretion was calculated as %ID. All feces and urine during the study period were collected for estimation of fraction and biological half-life of elimination. Cumulative excretion curves (urine and feces) were fitted from 0 to 168 hours with a function of the form:  $f_t = f^*(1 - \exp(-\lambda * t))$  using SigmaPlot® (Systat Software Inc, San Jose, CA) software. The ICRP 30 GI Model and Voiding Urinary Bladder Model in OLINDA|EXM were used to estimate the number of disintegrations occurring in the excretory organs. For gastrointestinal (GI) excretion, the fraction (f) entering at the small intestine was entered into the GI model module. For bladder excretion, the fraction passing bladder and biological half-life was entered in the Bladder Model. Activity in the remainder of the body was defined as the total injected activity minus the total excretion at any time (urine and feces) and activity in all individual organs evaluated. This activity was assumed to be uniformly distributed in the “remainder of the body.”

To estimate the absorbed dose for different tumor sizes ranging from 0.5 to 300 g mass, the mean value of total tumor nodules (%IA/g) obtained by mouse biodistribution study was directly fitted with exponential models to calculate the number of disintegrations, which again was input into OLINDA|EXM using the unit density sphere model.

## Maximum tolerated dose

The maximum tolerated dose (MTD) was defined as the activity dose below the dose resulting in either the death of any animal in groups of five animals or a body weight loss of more than 20%.<sup>23,24</sup> The toxicity radio-therapeutic <sup>188</sup>Re-liposome and chemo-therapeutic 5-FU was monitored by MTD study. Fifty male BALB/c mice were randomly grouped into cages of five mice (each mouse weighing 24.3 g on average). Mice were given 14.8, 22.2, 29.6, 37, and 44.4 MBq of <sup>188</sup>Re-liposomes and 90, 120, 150, 180, and 210 mg/kg of 5-FU in 200 μL by single intravenous injection, respectively. Mice were weighed twice per week, and the survival rate of the mice was recorded daily. The drug-induced toxicities (lethality and body weight loss) were determined for a minimum of 4 weeks.

## Therapeutic efficacy studies

At 7 days after intraperitoneal tumor cell inoculation, three groups of ten mice (each weighing 24.1 g on average) received



intravenous injections of 200  $\mu$ L <sup>188</sup>Re-liposomes (80% MTD, 29.6 MBq, and 0.88  $\mu$ mol phospholipid), 144 mg/kg (80% MTD) 5-FU dissolved in 200  $\mu$ L normal saline, and 200  $\mu$ L normal saline (control) respectively. Mice were checked for survival every day, and body weight was measured twice a week. The abdominal cavity was conscientiously inspected. The median survival time was carefully estimated using the Kaplan–Meier method of survival analysis for each treatment group. A Log-rank test was used to compare survival between treatment groups. The median survival time presented in the efficacy studies is calculated as the smallest survival time for which the survivor function is equal to 0.5.

To investigate the effects of <sup>188</sup>Re-liposomes on the tumor growth and ascites formation, 16 mice per group were intravenously treated with <sup>188</sup>Re-liposomes, 5-FU, and normal saline, respectively (doses as described above) at 7 days after intraperitoneal tumor cell inoculation. Four mice per group were sacrificed by CO<sub>2</sub> asphyxiation at 7, 9, 12, and 14 days after tumor inoculation. The abdominal cavity was conscientiously inspected. All ascites and tumor nodules were meticulously collected and weighed.

## Statistical analysis

Data were expressed as mean  $\pm$  standard error of the mean. SPSS 11 (SPSS Inc, Armonk, NY) software was used to perform statistical analysis, and the survival data were estimated by the Kaplan–Meier method and compared by Log-rank test. Values of  $P < 0.05$  were considered significant. The uptake value of drug in a tumor was compared by *t*-test. Values of  $P < 0.05$  were considered significant.

## Results

### Biodistribution studies of <sup>188</sup>Re-liposomes

The biodistribution of <sup>188</sup>Re-liposomes in the peritoneal carcinomatosis mouse model was studied at 1, 4, 24, 48, and 72 hours after intravenous injection and the results are summarized in Table 1. The <sup>188</sup>Re-liposomes in blood circulation were still at a high level of  $11.2\% \pm 1.17\%$  ID/g at 24 hours postinjection. Most normal organs reached the maximum levels at 4 hours postinjection. Uptakes of <sup>188</sup>Re-liposomes in normal organs were observed mainly in the spleen, kidney, and liver. Radioactivity in spleen, kidney, and liver reached the highest levels of  $10.4\% \pm 0.7\%$  ID/g,  $9.98\% \pm 0.45\%$  ID/g, and  $10.2\% \pm 0.57\%$  ID/g, respectively. After systemic administration of <sup>188</sup>Re-liposomes, radioactivity localized in ascites appeared at 1 hour and was maintained at higher levels from  $15.5\% \pm 0.74\%$  ID/g at 4 hours to  $10.8\% \pm 1.27\%$  ID/g at 24 hours. The radioactivity in

total tumor nodules rapidly accumulated to a high level of  $7.23\% \pm 1.39\%$  ID/g at 4 hours and progressively achieved a maximum of  $7.91\% \pm 2.02\%$  ID/g at 24 hours after intravenous administration of the <sup>188</sup>Re-liposomes. According to the anatomical studies, C26 tumor nodules spread throughout the peritoneal cavity, with most nodules appearing around the greater omentum, mesentery, diaphragm, and liver hilum at 10 days after inoculation. The uptakes of <sup>188</sup>Re-liposomes in tumor nodules collected from greater omentum, mesentery, and diaphragm were similar. Although the radioactivity in tumor nodules sampled from liver hilum was slightly less, there was no significant difference compared with levels from other implanted sites. The Tu to Mu ratio of <sup>188</sup>Re-liposomes reached  $30.6 \pm 9.3$  and  $25.8 \pm 6.1$  at 16 hours and 24 hours after injection, respectively. Very low levels of <sup>188</sup>Re-liposome uptake were noted in organs of the central nervous and musculoskeletal systems.

### Pharmacokinetics studies of <sup>188</sup>Re-liposome

The radioactivity–time curves from blood versus time points after intravenous injection of <sup>188</sup>Re-liposome are shown in Figure 1. Pharmacokinetic parameters in the peritoneal carcinomatosis mice model were estimated using WinNolin and a noncompartmental model ( $R_{sq} = 0.9554$ ), as summarized in Table 2. The maximum radioactivity ( $C_{max}$ ) in blood was determined as 47.1% ID/mL at 10 minutes for <sup>188</sup>Re-liposomes, which was also the  $T_{max}$  in the blood. The terminal half-life ( $T_{1/2\lambda z}$ ) of <sup>188</sup>Re-liposomes was 16.3 hours after intravenous injection. The  $AUC_{0 \rightarrow \infty}$  of <sup>188</sup>Re-liposomes was 820.4% ID/g\*h. The Cl of <sup>188</sup>Re-liposomes was 0.12 mL/h. The mean residence time ( $MRT_{0 \rightarrow \infty}$ ) of <sup>188</sup>Re-liposomes was 19.2 hours. These results revealed that <sup>188</sup>Re-liposomes exhibited high bioavailability and that long circulation of nanoliposome therapeutics was achieved in the peritoneal carcinomatosis mice model.

### Micro-SPECT/CT imaging and WBAR

To confirm the specific targeting of tumor sites and ascites of <sup>188</sup>Re-liposomes, microSPECT/CT imaging and WBAR were performed. The micro-SPECT/CT images of C26 tumor and ascites-bearing mice (on day 7 after tumor inoculation) acquired at different times after intravenous injection of <sup>188</sup>Re-liposomes are shown in Figure 2A. <sup>188</sup>Re-liposomes showed slow blood clearances and maintained a relatively higher activity in the abdominal cavity before 24 hours. Micro-SPECT/CT images showed a high uptake and targeting of <sup>188</sup>Re-liposomes in ascites and also in the tumor, liver, and feces. WBAR was

**Table 1** Biodistribution of  $^{188}\text{Re}$ -liposome after intravenous injection in C26 colonic peritoneal carcinomatosis mice

(%ID/g)	1 hour	4 hours	16 hours	24 hours	48 hours	72 hours
Whole blood	41.1 $\pm$ 0.32	36.1 $\pm$ 2.25	12.6 $\pm$ 0.45	11.2 $\pm$ 1.17	3.35 $\pm$ 0.81	1.43 $\pm$ 0.14
Brain	0.91 $\pm$ 0.06	0.68 $\pm$ 0.09	0.29 $\pm$ 0.01	0.27 $\pm$ 0.02	0.10 $\pm$ 0.02	0.05 $\pm$ 0.01
Skin	0.71 $\pm$ 0.07	0.87 $\pm$ 0.14	0.70 $\pm$ 0.15	0.80 $\pm$ 0.14	0.34 $\pm$ 0.06	0.44 $\pm$ 0.12
Muscle	0.39 $\pm$ 0.04	0.49 $\pm$ 0.13	0.26 $\pm$ 0.05	0.20 $\pm$ 0.04	0.11 $\pm$ 0.03	0.06 $\pm$ 0.01
Bone	2.06 $\pm$ 0.16	2.14 $\pm$ 0.19	1.04 $\pm$ 0.04	0.99 $\pm$ 0.05	0.35 $\pm$ 0.07	0.27 $\pm$ 0.06
Spleen	9.25 $\pm$ 0.37	10.4 $\pm$ 0.70	7.47 $\pm$ 0.35	7.63 $\pm$ 0.64	2.18 $\pm$ 1.05	1.41 $\pm$ 0.14
Small intestine	2.63 $\pm$ 0.55	3.98 $\pm$ 1.05	4.33 $\pm$ 1.28	4.70 $\pm$ 0.49	1.53 $\pm$ 0.66	0.78 $\pm$ 0.28
Large intestine	1.01 $\pm$ 0.11	1.39 $\pm$ 0.23	0.66 $\pm$ 0.26	1.01 $\pm$ 0.23	0.65 $\pm$ 0.12	0.36 $\pm$ 0.02
Kidney	9.24 $\pm$ 0.35	9.98 $\pm$ 0.45	4.16 $\pm$ 0.08	4.99 $\pm$ 0.79	1.56 $\pm$ 0.37	0.82 $\pm$ 0.04
Lung	7.80 $\pm$ 0.24	8.82 $\pm$ 0.71	3.15 $\pm$ 0.47	3.28 $\pm$ 0.39	1.21 $\pm$ 0.29	1.17 $\pm$ 0.44
Heart	3.57 $\pm$ 0.31	3.38 $\pm$ 0.20	1.47 $\pm$ 0.02	1.72 $\pm$ 0.15	0.65 $\pm$ 0.14	0.38 $\pm$ 0.04
Liver	9.63 $\pm$ 0.37	10.2 $\pm$ 0.57	6.60 $\pm$ 0.87	5.25 $\pm$ 1.65	1.99 $\pm$ 0.79	1.13 $\pm$ 0.41
Bladder	1.25 $\pm$ 0.24	1.43 $\pm$ 0.27	0.84 $\pm$ 0.15	0.83 $\pm$ 0.09	0.36 $\pm$ 0.04	0.36 $\pm$ 0.02
Pancreas	1.79 $\pm$ 0.33	2.32 $\pm$ 0.15	1.10 $\pm$ 0.10	0.56 $\pm$ 0.36	0.23 $\pm$ 0.08	0.16 $\pm$ 0.04
Stomach	1.38 $\pm$ 0.03	1.70 $\pm$ 0.12	1.75 $\pm$ 0.10	2.23 $\pm$ 0.35	0.80 $\pm$ 0.17	0.76 $\pm$ 0.22
Testes	0.74 $\pm$ 0.09	0.66 $\pm$ 0.04	0.50 $\pm$ 0.10	0.42 $\pm$ 0.07	0.22 $\pm$ 0.02	0.12 $\pm$ 0.00
Ascites	4.33 $\pm$ 0.54	15.5 $\pm$ 0.74	14.3 $\pm$ 0.69	10.8 $\pm$ 1.27	3.87 $\pm$ 0.86	1.61 $\pm$ 0.23
Metastases-1 <sup>a</sup>	4.92 $\pm$ 0.51	8.49 $\pm$ 1.70	7.88 $\pm$ 0.68	8.67 $\pm$ 2.13	3.35 $\pm$ 0.84	0.85 $\pm$ 0.11
Metastases-2 <sup>b</sup>	4.80 $\pm$ 1.11	3.40 $\pm$ 1.54	6.51 $\pm$ 0.37	3.69 $\pm$ 1.00	1.77 $\pm$ 0.45	1.06 $\pm$ 0.36
Metastases-3 <sup>c</sup>	5.51 $\pm$ 2.07	7.75 $\pm$ 1.12	5.02 $\pm$ 0.62	7.41 $\pm$ 2.78	0.68 $\pm$ 0.33	0.76 $\pm$ 0.10
Total tumor	5.05 $\pm$ 0.47	7.23 $\pm$ 1.39	7.36 $\pm$ 0.32	7.91 $\pm$ 2.02	3.26 $\pm$ 0.86	0.85 $\pm$ 0.11
Tu/Mu	13.8 $\pm$ 1.41	22.5 $\pm$ 6.29	30.6 $\pm$ 9.37	25.8 $\pm$ 6.11	25.9 $\pm$ 4.68	17.3 $\pm$ 5.26

**Notes:** Data were expressed as a percentage of injected dose per gram (%ID/g  $\pm$  standard error of the mean,  $n = 5$  at each time point); <sup>a</sup>metastases-1: tumor nodules in greater omentum, perisplenic, and mesentery; <sup>b</sup>metastases-2: in liver hilum; <sup>c</sup>metastases-3: in diaphragm.

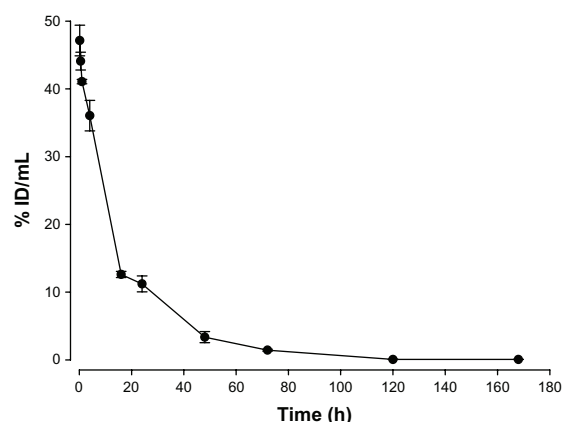
**Abbreviations:** Tu, tumor; Mu, muscle.

performed followed by the Micro-SPECT/CT scanning at 72 hours. The WBAR image also confirmed the tumor targeting of microSPECT/CT results as shown in Figure 2B, which is consistent with the biodistribution data (Table 1).

## Tissue radiation dose calculations

The radiation-absorbed dose projections for administration of  $^{188}\text{Re}$ -liposomes to humans, determined from the residence times in mice, are shown in Table 3. The fractions of the

$^{188}\text{Re}$ -liposomes excreted in the urinary and GI tract derived from accumulative urine and feces were 12% and 48% ID, respectively. That total excretion was 60% ID and was mostly through feces suggests the importance of hepatobiliary excretion for  $^{188}\text{Re}$ -liposomes. Lower doses were found, however, in other important therapy-limiting normal tissues such as the heart, lungs, liver, kidneys, and red marrow with values of 0.40 mSv/MBq, 0.17 mSv/MBq, 0.24 mSv/MBq, 0.20 mSv/MBq, and 0.04 mSv/MBq, respectively. The effective dose appears to

**Figure 1** Radioactivity–time curve of  $^{188}\text{Re}$ -liposomes in blood.

**Note:** Data are expressed as mean  $\pm$  SEM ( $n = 5$  at each time point).

**Abbreviations:** SEM, standard error of the mean; ID, injected dose.

**Table 2** Pharmacokinetic parameters of  $^{188}\text{Re}$ -liposome uptake after intravenous injection in C26 colonic peritoneal carcinomatosis mice

Parameter	$^{188}\text{Re}$ -liposomes
$T_{1/2\lambda z}$ (h)	16.3
$T_{max}$ (h)	0.16
$C_{max}$ (%ID/g)	47.1
Cl (mL/h)	0.12
$AUC_{(0 \rightarrow 168)}$ (%ID/g $\cdot$ h)	818.8
$AUC_{(0 \rightarrow \infty)}$ (%ID/g $\cdot$ h)	820.4
$MRT_{(0 \rightarrow \infty)}$ (h)	19.2

**Notes:** Values were calculated by mean of data ( $n = 5$ ) using WinNonlin (v 5.0.1; Pharsight Corp, Mountain View, CA) for a noncompartmental model.

**Abbreviations:**  $T_{max}$ , Time to achieve maximum concentration;  $C_{max}$ , maximum plasma concentration; Cl, clearance; %ID/g, percentage of the injected dose per gram of tissue;  $AUC_{(0 \rightarrow \infty)}$ , area under the tissue concentration–time curve from 0 h to infinity;  $MRT_{(0 \rightarrow \infty)}$ , mean residence time.

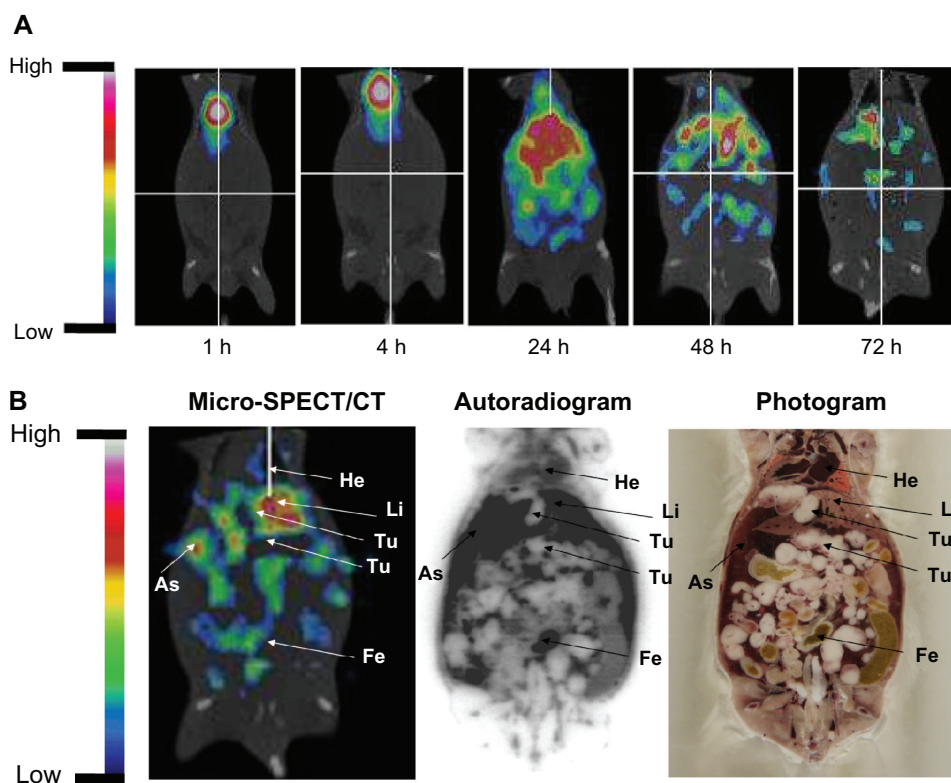


**Figure 2 (A)** The micro single-photon emission computed tomography (micro-SPECT/CT) of <sup>188</sup>Re-liposome-treated C26 peritoneal metastatic tumor-bearing mice. The <sup>188</sup>Re-liposomes, containing 12.95 MBq of <sup>188</sup>Re, were administered to each mouse by intravenous injection. Micro-SPECT images were acquired at 1, 4, 24, 48, and 72 hours after injection. **(B)** The whole-body autoradiography image was followed by micro-SPECT image acquisition at 72 hours after <sup>188</sup>Re-liposome injection, with the animal in the same position. Tumor nodules are indicated by arrows.

**Abbreviations:** Li, liver; As, ascites; He, heart; Fe, feces; Te, testis; Bl, bladder.

be approximately 0.80 mSv/MBq. Tumor radiation absorbed dose calculations are shown in Table 4. The unit density sphere model was used for calculation. Results revealed significantly greater absorption in tumor tissue than in normal organs. For a 10 g tumor, the estimated absorbed dose was 65.7 mSv/MBq.

## Therapeutic efficacy studies

In MTD study, the maximum dose with weight loss <20% of <sup>188</sup>Re-liposomes and 5-FU was determined to be 37 MBq and 180 mg/kg, respectively. In therapeutic efficacy studies, the 80% MTD of each drug was administered in each treatment group. Table 3 summarizes the therapeutic efficacy for each group receiving different treatments at 7 days after tumor inoculation. The survival curves for different treatment groups are shown in a Kaplan–Meier plot in Figure 3. Mice were treated at 7 days after tumor inoculation ( $n = 10$  for each group). The median survival time for the control mice, who received normal saline, was 24.3 days (Table 5). The median survival times for the mice treated with <sup>188</sup>Re-liposomes (29.6 MBq) and 5-FU (144 mg/kg) were 32.8 and 26.7 days, respectively. The results of the median survival time of the radiotherapeutics of <sup>188</sup>Re-liposomes were statistically different from the chemotherapeutics of

5-FU ( $P = 0.03$ ). The therapeutic studies demonstrated better survival time and therapeutic efficacy for mice who received intravenously administered <sup>188</sup>Re-liposomes. The  $P$  values for the differences among the survival curves of the various treatment groups are shown in Table 5.

## Tumor and ascites inhibition studies

The first macroscopic C26 tumor deposits in the peritoneal cavity were observed 5 days after intraperitoneal inoculation. Tumor deposits were small (1–3 mm in diameter) and mostly located in the upper abdomen in the great omentum and adjacent to the spleen. At 7–10 days after tumor inoculation, C26 tumor nodules had formed throughout the peritoneal cavity, with most nodules appearing in the great omentum, liver hilum, mesentery, and diaphragm; ascites also formed. All visible tumor nodules and ascites were sampled and weighed during postmortem examination. The weights of the tumors and ascites are presented as the initial weights at 7 days after tumor inoculation for different groups. After <sup>188</sup>Re-liposomes and 5-FU were administered at 7 days after tumor inoculation, significantly large inhibitions of hemorrhagic ascites formation and tumor growth were observed

**Table 3** Radiation dose estimates for  $^{188}\text{Re}$ -liposome in humans

Organ	Estimated dose (mSv · MBq <sup>-1</sup> )*
Adrenals	5.75E-02
Brain	1.51E-02
Breasts	5.54E-02
Gallbladder wall	6.26E-02
LLI wall	5.78E000
Small intestine	1.05E000
Stomach wall	7.68E-02
ULI wall	3.85E000
Heart wall	4.02E-01
Kidneys	1.99E-01
Liver	2.40E-01
Lungs	1.65E-01
Muscle	1.35E-02
Ovaries	7.00E-02
Pancreas	4.39E-02
Red marrow	4.20E-02
Osteogenic cells	1.49E-01
Skin	5.51E-02
Spleen	2.58E-01
Testes	1.96E-02
Thymus	5.63E-02
Thyroid	5.53E-02
Urinary bladder wall	1.69E-01
Uterus	6.34E-02
Total body	1.10E-01
Effective dose	7.98E-01

**Notes:** \*Radiation-absorbed dose projections in humans were determined from residence times for  $^{188}\text{Re}$ -liposomes in mice bearing C26 peritoneal metastatic tumor and were calculated by use of OLINDA|EXM® (v 1.0; Vanderbilt University, Nashville, TN).

**Abbreviations:** LLI, lower large intestine; ULI, upper large intestine.

in the  $^{188}\text{Re}$ -liposome-treated group in comparison with the 5-FU at 9–14 days (ascites: decrease of 83.3% and 44.9% at 14 days for  $^{188}\text{Re}$ -liposome-treated group and 5-FU-treated group, respectively; tumor: decrease of 63.4% and 9.1% at 14 days, respectively;  $P < 0.05$ ) (Figure 4). To address the inhibition property of  $^{188}\text{Re}$ -liposomes in different metastatic sites, tumor nodules were precisely sampled from the greater omentum, mesentery, liver hilum, and diaphragm.

**Table 4** Absorbed doses of  $^{188}\text{Re}$ -liposomes in sphere tumor derived from C26 peritoneal metastatic tumor

Sphere Mass (g)	Estimated dose (mSv · MBq <sup>-1</sup> )*
0.5	1110
1	588
4	159
10	65.7
40	17.0
100	6.91
300	2.34

**Notes:** Radiation-absorbed dose projections in humans were determined from residence times for  $^{188}\text{Re}$ -liposomes in mice bearing C26 peritoneal metastatic tumors and were calculated using OLINDA|EXM® (v 1.0; Vanderbilt University, Nashville, TN).

$^{188}\text{Re}$ -liposomes had significantly inhibited tumor growths in these implanted sites. Moreover, in comparison with 5-FU,  $^{188}\text{Re}$ -liposomes demonstrated greater inhibition of the tumor growths in mesentery and liver hilum (mesentery: decrease of 61.3% and 12.8% at 14 days for  $^{188}\text{Re}$ -liposome-treated group and 5-FU-treated group, respectively; liver hilum: decrease of 87.1% and 5.9% at 14 days, respectively;  $P < 0.05$ ) (Figure 5). These results demonstrate better therapeutic efficacy in the inhibition of the progression in peritoneal carcinomatosis for mice that received intravenously administered  $^{188}\text{Re}$ -liposomes.

## Discussion

Most cases with peritoneal carcinomatosis have no satisfactory response to systemic chemotherapy.<sup>8</sup> The main reason for this lack of success is that cytostatic drugs administered intravenously do not affect tumors of peritoneal metastases with a sufficiently high concentration.<sup>25</sup> Little previous research has evaluated the therapeutic efficacy of radionuclide-conjugated liposomes administered intravenously in advanced metastatic colorectal cancer. Colorectal cancer frequently gives rise to the intraperitoneal spread of tumor cells and multiple metastatic tumor nodules are a result of peritoneal carcinomatosis. Initially, these nodules are small volume, with marked neovascularization in the infiltrate sites.<sup>26</sup> The tumor-associated vascularization with high permeability is favorable for targeting by liposomal drugs by EPR effect. Therefore, ascertaining the efficacy of passively nanotargeted  $^{188}\text{Re}$ -liposomes via the intravenous route in peritoneal carcinomatosis of colorectal origin was worthwhile.

Biodistribution results confirmed the significantly high uptake in tumor tissues and that long blood circulation favored the use of  $^{188}\text{Re}$ -liposomes by systemic route in treating peritoneal carcinomatosis. In the authors' previous report, the biodistribution, and pharmacokinetics of intraperitoneal injected  $^{188}\text{Re}$ -liposomes in a peritoneal carcinomatosis mouse model were studied.<sup>27,28</sup> Compared with the current results, both administration routes exhibited prolonged retention of  $^{188}\text{Re}$ -liposomes within the ascites and tumors. In addition, they achieved the highest uptake of radioactivity in tumor tissues at 24-hours postinjection with a similar level ( $7.91\% \pm 2.02\%$  intravenous ID/g versus  $6.57\% \pm 1.71\%$  intraperitoneal ID/g). However, intravenous injection of  $^{188}\text{Re}$ -liposomes resulted in faster accumulation in tumor tissues than intraperitoneal injection:  $7.23 \pm 1.39$  ID/g and  $3.34 \pm 1.24$  ID/g at 4 hours after injection, respectively. The level of radioactivity of  $^{188}\text{Re}$ -liposomes in blood was



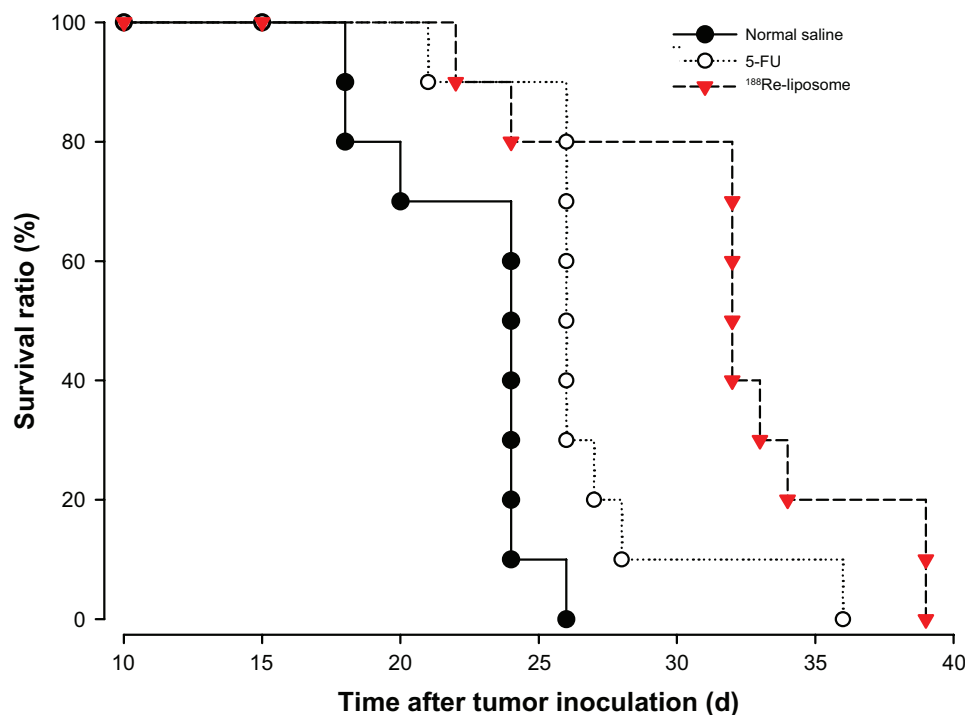


**Figure 3** Kaplan–Meier survival curves for mice bearing C26 peritoneal metastatic tumor after administration of <sup>188</sup>Re-liposomes (29.6 MBq, ▼), 5-FU (144 mg/kg, ○), and normal saline (●) by single intravenous injection. Mice were treated 7 days after tumor inoculation.

**Note:** n = 10 for each group.

maintained at relatively steady high levels for 24 hours after intravenous injection (Table 1).

It was noticed that after the redistribution of systemic circulation, more than 10% ID/g was recovered in the ascitic fluid over 4–24 hours. The presence of intravenous-injected <sup>188</sup>Re-liposomes in the peritoneal cavity may be associated with increased permeability of the tumor and peritoneal microvasculature. Previous studies with ascitic tumors demonstrate a steady extravasation process of liposomes into the ascitic fluid with gradual release of the drug followed by drug diffusion into the ascitic cellular compartment.<sup>29,30</sup> This accumulation process has been shown to be related

to the characteristics of the liposomes: small liposomes (with mean diameters of approximately 100 nm) achieve efficient accumulation in the peritoneal cavity in ascitic, tumor-bearing animals after intravenous injection.<sup>29</sup> The authors' results suggest that the peritoneal cavity serves as an appropriate extravascular site for the passive targeting of <sup>188</sup>Re-liposomes in peritoneal carcinomatosis. <sup>188</sup>Re-liposomes intravenously administered not only rapidly target tumor tissues by EPR effect but also provide an extravasated pool of highly concentrated <sup>188</sup>Re-liposomes surrounding the tumor nodules. The prolonged exposure of tumor to <sup>188</sup>Re-liposomes by both mechanisms may account for the superior therapeutic effect observed in the experiments reported here.

In the authors' previous studies, the biodistribution and pharmacokinetic properties of unencapsulated <sup>188</sup>Re-BMEDA had been evaluated in a mouse model with C26 colon solid tumor and peritoneal carcinomatosis, respectively.<sup>22,27</sup> The results showed no evidence for the accumulation of <sup>188</sup>Re-BMEDA in tumors or in any normal organs. The fast blood clearance and excretion of <sup>188</sup>Re-BMEDA were observed. Compared with the present study, <sup>188</sup>Re-liposomes exhibited significant targeting and retention in the tumor. Pharmacokinetic study showed the slow clearance rate of <sup>188</sup>Re-liposomes and the AUC was 4.7-fold greater

**Table 5** Comparative therapeutic efficacy of different treatments at 7 days after intraperitoneal C26 peritoneal metastatic tumor inoculation

Group	Median survival time (d)	% ILS <sup>a</sup>	Significance P value
<sup>188</sup> Re-liposome (29.6 MBq)	32.8	34.6	0.0006 <sup>b</sup> , 0.03 <sup>c</sup>
5-FU (144 mg/kg)	26.7	9.6	0.001 <sup>b</sup>
Normal saline (control)	24.3	—	—

**Notes:** <sup>a</sup>% increase in life span (% ILS) is expressed as  $(T/C - 1) \times 100\%$ , where T is the median survival time of treated mice and C is the median survival time of control mice; <sup>b</sup>P values versus control were determined by use of Log-rank test (significant variation,  $P < 0.01$ ); <sup>c</sup>P values vs 5-FU were determined by use of Log-rank test (significant variation,  $P < 0.05$ ).

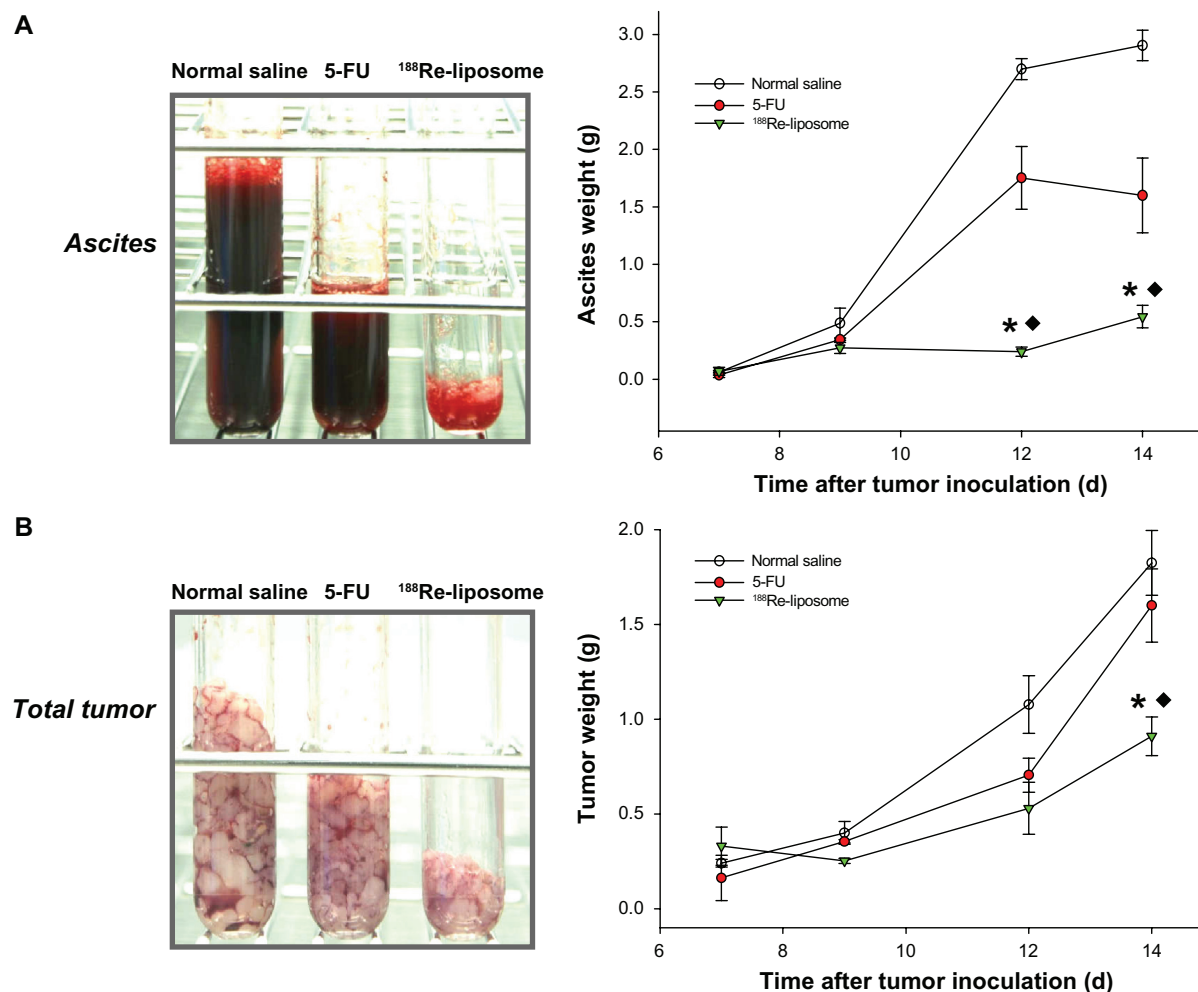


**Figure 4** The total ascites (A) and tumors (B) were sampled in the tubes and weighed at 0, 2, 4, and 7 days after administration of  $^{188}\text{Re}$ -liposomes (29.6 MBq, ▼), 5-FU (144 mg/kg, ●), and normal saline (○), respectively, by single intravenous injection.

**Notes:** Data are expressed as mean  $\pm$  SEM ( $n = 4$  mice/group/time point); \*significant difference between  $^{188}\text{Re}$ -liposome- and normal saline-treated groups; ♦ significant difference between  $^{188}\text{Re}$ -liposome- and 5-FU-treated groups.

**Abbreviation:** SEM, standard error of the mean.

than that of  $^{188}\text{Re}$ -BMEDA. These results suggested that pegylated nanoliposomes have higher bioavailability than  $^{188}\text{Re}$ -BMEDA, and the transportation of passive-targeted liposomes loaded with  $^{188}\text{Re}$ -BMEDA on tumor sites was achieved.

In vivo and noninvasive molecular imaging such as positron emission tomography (PET), single photon emission computed tomography (SPECT), magnetic resonance imaging, and optical imaging have gradually expanded to drug discovery and development in preclinical studies.<sup>31–33</sup> In this study, in vivo direct visualization of tumor and ascites targeting and distribution of  $^{188}\text{Re}$ -liposomes were evaluated in peritoneal carcinomatosis mice by micro-SPECT/CT imaging, which provides further information for in vivo tumor and ascites retention (Figure 2). The information from micro-SPECT/CT imaging is also supported by whole-body

autoradiography and biodistribution data. An intraperitoneal ovarian cancer nude rat model was previously studied with in vivo microPET imaging, and the study found that ascites gathered from tumor-bearing rats had higher fludeoxyglucose uptake than the peritoneal fluid collected from control rats, which is similar to the results of the present study.<sup>34</sup>

Optimized radionuclide therapy for cancer treatment is based on the concept of absorbed dose to the dose limiting normal organ or tissue, and either red marrow or the liver may be the dose-limiting critical organ for radionuclide pegylated nanoliposome therapy.<sup>35</sup> Macey and Meredith projected  $^{188}\text{Re}$  as the most advantageous of the  $\beta$  emitters for a favorable tumor/marrow ratio.<sup>36</sup> In the present authors' dosimetry study, the absorbed doses to liver, red marrow, and total body with intravenous injection were 0.24, 0.04, and 0.11 mSv/MBq for  $^{188}\text{Re}$ -liposomes (Table 3), which were

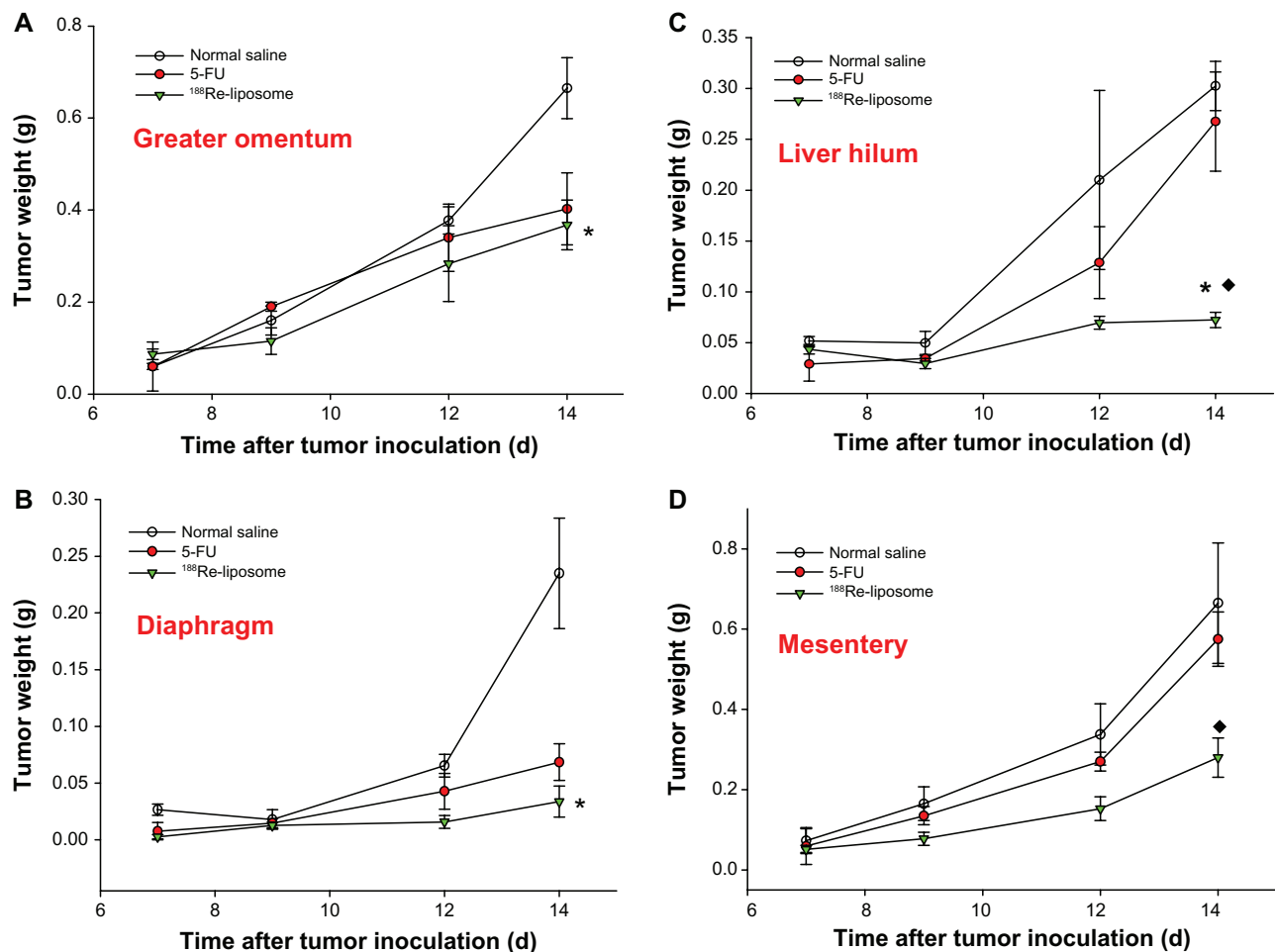


**Figure 5** The total tumor nodules derived from (A) greater omentum, (B) diaphragm, (C) liver hilum, and (D) mesentery were sampled in the tubes and weighed at 0, 2, 4, and 7 days after administration of  $^{188}\text{Re}$ -liposomes (29.6 MBq, ▼), 5-FU (144 mg/kg, ●), and normal saline (○), respectively, by single intravenous injection.

**Notes:** Data are expressed as mean  $\pm$  SEM ( $n = 4$  mice/group/time point); \*significant difference between  $^{188}\text{Re}$ -liposome and 5-FU-treated groups; ◆ significant difference between  $^{188}\text{Re}$ -liposome and normal saline-treated groups.

**Abbreviation:** SEM, standard error of the mean.

lower than those reported by Emfietzoglou et al (of 0.44, 0.12, and 0.15 mSv/MBq, respectively), for an  $^{188}\text{Re}$ -labeled small unilamellar vesicle liposome.<sup>19</sup> According to the present authors' dosimetry results, red marrow was regarded as the primary critical organ for  $^{188}\text{Re}$ -liposomes. This low-absorbed dose of red marrow for  $^{188}\text{Re}$ -liposomes allows the maximized activity of  $^{188}\text{Re}$ -liposomes to be administrated for achieving the highest absorbed dose to tumors.

Safra et al report that tumor size is an important prognostic factor for therapeutic response to the liposomal drug doxorubicin in ovarian cancer, which suggests that the tumor volume is clinically relevant for liposome uptake.<sup>37</sup> The trend is that the liposome uptake is higher in smaller tumors,<sup>38,39</sup> which is consistent with Harrington's findings in animal tumor models.<sup>40</sup> The effect of tumor size on the tumor-absorbed dose of  $^{188}\text{Re}$ -liposomes was also calculated using OLINDA|EXM (Table 4). The results showed that the

tumor-absorbed dose decreased almost ninefold for tumors between 1 and 10 g (588 mSv/MBq and 65.7 mSv/MBq, respectively) and 85-fold with tumor mass changing from 1 to 100 g (588 mSv/MBq and 6.91 mSv/MBq, respectively) for  $^{188}\text{Re}$ -liposomes. These results indicate that small tumors could receive a higher absorbed dose than larger tumors and reflect one of the advantages of  $^{188}\text{Re}$ -liposomes in treating peritoneal carcinomatosis with multiple small-volume tumor nodules. It is also suggested that  $^{188}\text{Re}$ -liposomes may have the potential to be applied in adjuvant treatment combined with cytoreductive surgery to eliminate residual tumor nodules.

Intraperitoneal inoculation of tumor cells in an animal model is a commonly used method to induce peritoneal carcinomatosis.<sup>41</sup> The tumor progressive patterns in the mouse model discussed here also mimic the pathological features seen in clinical practice, including preferential seeding to

the greater omentum and the development of hemorrhagic ascites.<sup>3</sup> The authors' treatments were administered at 7 days after tumor inoculation to evaluate the therapeutic efficacy in the early stages of peritoneal carcinomatosis. Significantly improved therapeutic efficacy of <sup>188</sup>Re-liposomes in treating peritoneal carcinomatosis was revealed in the present study. It was shown that internal radiotherapy with <sup>188</sup>Re-liposomes achieved the best curative effects, including extended lifespan (increase of 34.6%; Table 5), reduced production of ascites (decrease of 83.3% at 14 days; Figure 4A), and inhibited tumor growth (decrease of 63.4% at 14 days; Figure 4B). These results are significantly better than those seen after treatment with 5-FU chemotherapy and in the vehicle group of normal saline.

It should be noted that significant inhibition of ascites formation was observed in the <sup>188</sup>Re-liposome-treated group for the period of peritoneal metastatic progression (Figure 4A). The presentation of ascites in association with colonic carcinoma has been attributed to metastases. However, the large accumulation of ascites is also considered a prominent factor contributing to the large incidence of further spread of tumor implants in peritoneal cavity.<sup>3</sup> Therefore, the management of patients with ascites is important, not only for improving quality of life but also for restricting metastatic progression.<sup>42</sup> Moreover, <sup>188</sup>Re-liposomes exhibited greater antitumor activity than 5-FU in all the metastatic sites collected, especially in the liver hilum and mesentery (Figure 5C and D). In <sup>188</sup>Re-liposome-treated mice, it was found that most of the tumor nodules clustered in the greater omentum, rather than spreading to multiple implanted sites as in the 5-FU-treated group. These observations suggested that the <sup>188</sup>Re-liposome treatment is more effective in inhibiting tumor growth and further dissemination in peritoneal carcinomatosis than 5-FU.

## Conclusion

The present study demonstrates the advantages of intravenously administrated <sup>188</sup>Re-liposomes in treating peritoneal carcinomatosis in a mouse model. The biodistribution, pharmacokinetics, and imaging studies of <sup>188</sup>Re-liposomes in the peritoneal carcinomatosis model revealed good tumor and ascites targeting, bioavailability, and localization. The dosimetry study also provides safety information for <sup>188</sup>Re-liposomes in further clinical applications. In a therapeutic study, <sup>188</sup>Re-liposomes were found to achieve apparent curative ability, including inhibition of the tumor cell proliferation and further dissemination, and malignant

ascites formation. The results presented here establish the potential of <sup>188</sup>Re-liposomes for the treatment of peritoneal carcinomatosis.

## Acknowledgment

The authors thank Dr TY Luo and CJ Liu for providing the rhenium-188.

## Disclosure

The authors declare no conflicts of interest in relation to this paper.

## References

1. Eisenberg B, Decosse JJ, Harford F, Michalek J. Carcinoma of the colon and rectum: the natural history reviewed in 1704 patients. *Cancer*. 1982;49(6):1131–1134.
2. Gallagher DJ, Kemeny N. Metastatic colorectal cancer: from improved survival to potential cure. *Oncology*. 2010;78(3–4):237–248.
3. Carmignani CP, Sugarbaker TA, Bromley CM, Sugarbaker PH. Intraperitoneal cancer dissemination: mechanisms of the patterns of spread. *Cancer Metastasis Rev*. 2003;22(4):465–472.
4. Pestieau SR, Sugarbaker PH. Treatment of primary colon cancer with peritoneal carcinomatosis: comparison of concomitant vs delayed management. *Dis Colon Rectum*. 2000;43(10):1341–1346; discussion 1347–1348.
5. Sood R. Ascites: Diagnosis and Management. *JACM*. 2000;5(1):81–89.
6. Hegde SR, Sun W, Lynch JP. Systemic and targeted therapy for advanced colon cancer. *Expert Rev Gastroenterol Hepatol*. 2008;2(1):135–149.
7. Wolpin BM, Mayer RJ. Systemic treatment of colorectal cancer. *Gastroenterology*. 2008;134(5):1296–1310.
8. Gomez Portilla A, Cendoya I, Lopez de Tejada I, et al. Peritoneal carcinomatosis of colorectal origin. Current treatment. Review and update. *Rev Esp Enferm Dig*. 2005;97(10):716–737.
9. Novotny-Diermayr V, Sangthongpitak K, Hu CY, et al. SB939, a novel potent and orally active histone deacetylase inhibitor with high tumor exposure and efficacy in mouse models of colorectal cancer. *Mol Cancer Ther*. 2010;9(3):642–652.
10. Gil-Ad I, Zolotov A, Lomnitski L, et al. Evaluation of the potential anti-cancer activity of the antidepressant sertraline in human colon cancer cell lines and in colorectal cancer-xenografted mice. *Int J Oncol*. 2008;33(2):277–286.
11. Petros RA, DeSimone JM. Strategies in the design of nanoparticles for therapeutic applications. *Nat Rev Drug Discov*. 2010;9(8):615–627.
12. Allen TM, Cullis PR. Drug delivery systems: entering the mainstream. *Science*. 2004;303(5665):1818–1822.
13. Torchilin VP. Recent advances with liposomes as pharmaceutical carriers. *Nat Rev Drug Discov*. 2005;4(2):145–160.
14. Newman MS, Colbern GT, Working PK, Engbers C, Amantea MA. Comparative pharmacokinetics, tissue distribution, and therapeutic effectiveness of cisplatin encapsulated in long-circulating, pegylated liposomes (SPI-077) in tumor-bearing mice. *Cancer Chemother Pharmacol*. 1999;43(1):1–7.
15. Vaage J, Donovan D, Wipff E, et al. Therapy of a xenografted human colonic carcinoma using cisplatin or doxorubicin encapsulated in long-circulating pegylated stealth liposomes. *Int J Cancer*. 1999;80(1):134–137.
16. Uldrick TS, Whitby D. Update on KSHV epidemiology, Kaposi Sarcoma pathogenesis, and treatment of Kaposi Sarcoma. *Cancer Lett*. 2011;305(2):150–162.



17. Gonzalez Martin A. Safety profile of trabectedin in combination with liposomal pegylated doxorubicin in relapsed ovarian carcinoma: considerations for optimal management. *Int J Gynecol Cancer*. 2011;21(10 Suppl 1):S6–S8.
18. Cobleigh MA. Other options in the treatment of advanced breast cancer. *Semin Oncol*. 2011;38(Suppl 2):S11–S16.
19. Emfietzoglou D, Kostarelos K, Sgouros G. An analytic dosimetry study for the use of radionuclide-liposome conjugates in internal radiotherapy. *J Nucl Med*. 2001;42(3):499–504.
20. Ting G, Chang CH, Wang HE. Cancer nanotargeted radiopharmaceuticals for tumor imaging and therapy. *Anticancer Res*. 2009;29(10):4107–4118.
21. Tseng YL, Hong RL, Tao MH, Chang FH. Sterically stabilized anti-idiotype immunoliposomes improve the therapeutic efficacy of doxorubicin in a murine B-cell lymphoma model. *Int J Cancer*. 1999;80(5):723–730.
22. Chang YJ, Chang CH, Chang TJ, et al. Biodistribution, pharmacokinetics and microSPECT/CT imaging of <sup>188</sup>Re-BMEDA-liposome in a C26 murine colon carcinoma solid tumor animal model. *Anticancer Res*. 2007;27(4B):2217–2225.
23. Cao S, Rustum YM. Synergistic antitumor activity of irinotecan in combination with 5-fluorouracil in rats bearing advanced colorectal cancer: role of drug sequence and dose. *Cancer Res*. 2000;60(14):3717–3721.
24. Moore M, Hirte HW, Siu L, et al. Phase I study to determine the safety and pharmacokinetics of the novel Raf kinase and VEGFR inhibitor BAY43-9006, administered for 28 days on/7 days off in patients with advanced, refractory solid tumors. *Ann Oncol*. 2005;16(10):1688–1694.
25. Yonemura Y, Fujimura T, Fushida S, et al. Hyperthermo-chemotherapy combined with cytoreductive surgery for the treatment of gastric cancer with peritoneal dissemination. *World J Surg*. 1991;15(4):530–535; discussion 535–536.
26. Jayne D. Molecular biology of peritoneal carcinomatosis. *Cancer Treat Res*. 2007;134:21–33.
27. Chen LC, Chang CH, Yu CY, et al. Biodistribution, pharmacokinetics and imaging of <sup>188</sup>Re-BMEDA-labeled pegylated liposomes after intraperitoneal injection in a C26 colon carcinoma ascites mouse model. *Nucl Med Biol*. 2007;34(4):415–423.
28. Chen LC, Chang CH, Yu CY, et al. Pharmacokinetics, micro-SPECT/CT imaging and therapeutic efficacy of <sup>188</sup>Re-DXR-liposome in C26 colon carcinoma ascites mice model. *Nucl Med Biol*. 2008;35(8):883–893.
29. Bally MB, Masin D, Nayar R, Cullis PR, Mayer LD. Transfer of liposomal drug carriers from the blood to the peritoneal cavity of normal and ascitic tumor-bearing mice. *Cancer Chemother Pharmacol*. 1994;34(2):137–146.
30. Gabizon AA. Selective tumor localization and improved therapeutic index of anthracyclines encapsulated in long-circulating liposomes. *Cancer Res*. 1992;52(4):891–896.
31. Massoud TF, Gambhir SS. Molecular imaging in living subjects: seeing fundamental biological processes in a new light. *Genes Dev*. 2003;17(5):545–580.
32. Chang CH, Wang HE, Wu SY, et al. Comparative evaluation of FET and FDG for differentiating lung carcinoma from inflammation in mice. *Anticancer Res*. 2006;26(2A):917–925.
33. Chang CH, Jan ML, Fan KH, et al. Longitudinal evaluation of tumor metastasis by an FDG-microPET/microCT dual-imaging modality in a lung carcinoma-bearing mouse model. *Anticancer Res*. 2006;26(1A):159–166.
34. Zavaleta CL, Phillips WT, Bradley YC, McManus LM, Jerabek PA, Goins BA. Characterization of an intraperitoneal ovarian cancer xenograft model in nude rats using noninvasive microPET imaging. *Int J Gynecol Cancer*. 2007;17(2):407–417.
35. Fisher DR. Assessments for high dose radionuclide therapy treatment planning. *Radiat Prot Dosimetry*. 2003;105(1–4):581–586.
36. Macey DJ, Meredith RF. A strategy to reduce red marrow dose for intraperitoneal radioimmunotherapy. *Clin Cancer Res*. 1999;5(10 Suppl):3044s–3047s.
37. Safra T, Groshen S, Jeffers S, et al. Treatment of patients with ovarian carcinoma with pegylated liposomal doxorubicin: analysis of toxicities and predictors of outcome. *Cancer*. 2001;91(1):90–100.
38. Harrington KJ, Mohammadtaghi S, Uster PS, et al. Effective targeting of solid tumors in patients with locally advanced cancers by radiolabeled pegylated liposomes. *Clin Cancer Res*. 2001;7(2):243–254.
39. Lim HJ, Masin D, McIntosh NL, Madden TD, Bally MB. Role of drug release and liposome-mediated drug delivery in governing the therapeutic activity of liposomal mitoxantrone used to treat human A431 and LS180 solid tumors. *J Pharmacol Exp Ther*. 2000;292(1):337–345.
40. Harrington KJ, Rowlinson-Busza G, Syrigos KN, et al. Influence of tumour size on uptake of <sup>111</sup>In-DTPA-labelled pegylated liposomes in a human tumour xenograft model. *Br J Cancer*. 2000;83(5):684–688.
41. Sugarbaker PH. Observations concerning cancer spread within the peritoneal cavity and concepts supporting an ordered pathophysiology. *Cancer Treat Res*. 1996;82:79–100.
42. Adam RA, Adam YG. Malignant ascites: past, present, and future. *J Am Coll Surg*. 2004;198(6):999–1011.

## International Journal of Nanomedicine

### Publish your work in this journal

The International Journal of Nanomedicine is an international, peer-reviewed journal focusing on the application of nanotechnology in diagnostics, therapeutics, and drug delivery systems throughout the biomedical field. This journal is indexed on PubMed Central, MedLine, CAS, SciSearch®, Current Contents®/Clinical Medicine,

Submit your manuscript here: <http://www.dovepress.com/international-journal-of-nanomedicine-journal>

Dovepress

Journal Citation Reports/Science Edition, EMBASE, Scopus and the Elsevier Bibliographic databases. The manuscript management system is completely online and includes a very quick and fair peer-review system, which is all easy to use. Visit <http://www.dovepress.com/testimonials.php> to read real quotes from published authors.